Available online at www.CivileJournal.org

Civil Engineering Journal

(E-ISSN: 2476-3055; ISSN: 2676-6957)

Vol. 9, No. 02, February, 2023

Multigene Genetic Programming Based Prediction of Concrete Fracture Parameters of Unnotched Specimens

M. R. Sudhir [1*], M. Beulah [1]

[1] *Department of Civil Engineering, School of Engineering & Technology, CHRIST (Deemed to be University), Bangalore, India.*

Received 14 November 2022; Revised 14 January 2023; Accepted 21 January 2023; Published 01 February 2023

Abstract

This study explores the fracture energy of notched and unnotched concrete specimens subjected to the classical three-point bend test, instantiating a gradational step in the continued development of concrete fracture mechanics. An experimental campaign involving 18 notched test specimens and nine unnotched specimens of three different grades of concrete, an examination of the existing literature models for unnotched specimens, and a novel Multigene Genetic programming (MGGP) based concrete fracture energy model for unnotched specimens are integral to this study. As a salient result, the multiple approaches to quasi-brittle materials adopted in the study, highlighted the criticality of the determination of fracture energy, tensile strength and characteristic length for the crack width study. The failure modes of notched and unnotched specimens were found to be similar. The reported literature has mainly focused on a limited number of fracture energy influencing parameters. Therefore, six impact parameters have been chosen and incorporated into the present study to provide a more acceptable explanation of concrete fracture behaviour. A sensitivity analysis of the parameters and an error analysis of the model undertaken have established the accuracy and robustness of the developed MGGP model.

Keywords: Concrete; Fracture Parameters; Notched and Unnotched Specimens; Multigene Genetic Programming.

1. Introduction

The fracture mechanics principles have been applied to quasi-brittle materials like concrete to understand structural members' service performance and failure analysis. The toughness of concrete is related to the energy required to initiate and propagate a crack until failure. The concrete fracture characterization is complex as concrete has heterogeneous composition. Karihaloo et al. (2003) [1] carried out a series of experiments to examine the size dependency of TPB notched and unnotched specimens for both normal strength concrete (NSC) and high strength concrete (HSC). Abdalla & Karihaloo (2004) [2] hypothesized that both true fracture energy and corresponding softening relations were necessary for the analysis of cracked concrete structures by undertaking fracture tests conducted on TPB and wedge split concrete specimens. Luigi & Gianluca (2008) [3] focused on the fracture parameters of concrete through experimentation to arrive at the fracture energy and tensile strength of the specimens. Raghu Prasad (2009) [4] and Muralidhara (2010) [5] performed TPB tests on geometrically similar specimens. Skarzynski & Tejchman (2010) [6] used finite element analysis (FEA) and the DIC method to postulate on the FPZ of notched concrete specimens under TPB. Ince & Cetin (2019) [7] reported that the fracture parameters of concrete were influenced by compressive strength, maximum aggregate size, water-cement ratio, and aggregate type in testing.

The toughness was considered to be a material property along with the strain-energy release rate, [8] and characteristic length as a measure of brittleness [9]. The determination of the concrete fracture behaviour was facilitated by ascertaining tensile strength, fracture energy, and modulus of elasticity. The flexural tensile strength for unnotched

* Corresponding author: colonel.sudhir@christuniversity.in

http://dx.doi.org/10.28991/CEJ-2023-09-02-011

specimens was experimentally determined by the three-point bend test [10]. The deadweight deflection was added to the RILEM fracture energy equation [11]. The concrete fracture energy was modeled by Wittman et al. (1978) [12]. Actual crack formation in a concrete specimen required a certain amount of energy called the fracture energy, and the value of it was computed. Also, the size effect was the most compelling reason for employing fracture mechanics principles in concrete designs [13]. The fracture energy of concrete as a function of the grade of concrete, compressive strength, and temperature was determined [14]. An understanding of the concrete softening curve was developed using two critical parameters, tensile strength and fracture energy [15]. The characteristic length (L_{ch}) was related to the strength of the unnotched and notched test specimens [16]. Fracture energy of test specimens was found to be higher for low water-cement ratios than for those specimens with high water-cement ratios [17], and this was in agreement with the observations of Peterson (1980) [18] and Wittman et al. (1987) [12]. However, it was pointed out that additional test series on unnotched specimens with a wide range of cross-section heights should be carried out experimentally in the future [19]. The fracture energy, G_f, depended primarily on the water-cement ratio, the aggregate type, the maximum aggregate size, the age of the concrete, and the curing conditions [20]. As Wittman's model predicted higher fracture energy values, the authors provided a realistic model for the prediction of concrete fracture energy [21].

The authors opined that more unnotched specimen tests with various cross sections were required for fracture parameter estimation. They concluded that the size effect coefficient could be directly calculated from the modulus of rupture [22]. The fracture energy of concrete was size dependent and for non-linear models, two fracture parameters were needed to define the concrete fracture behaviour [23]. The water-cement ratio (w/c) had a significant bearing on the interfacial transition zone between concrete paste and aggregate, thereby affecting the strength of concrete [24]. The fracture energy of concrete was investigated to ascertain the effects of w/c, coarse aggregate type, and curing temperature for certain generalised conclusions [25]. The computations of concrete's characteristic length and tensile strength were founded on energy equivalence [26]. Heuristics methods such as the genetic algorithm were concluded to be powerful tools to solve problems involving uncertainties [27]. To understand the fracture properties of concrete, cement mortar was tested, and it was found that the water-cement ratio and cement grade have major influences on the fracture behaviour [28]. A series of notched and unnotched square specimens were tested for the developed two-parameter model, and the maximum fracture loads were investigated [29]. A theoretical model was developed for the fracture toughness of concrete using unnotched specimens, which studied the effects of aggregate size [30]. Splitting strips were employed for determining the fracture behavior of quasi-brittle materials in square specimens with edge cracks. The experimentation adopted a two-parameter model for research inferences [31]. Notched specimens of fiber-reinforced concrete in flexure were subjected to cyclic loads, and the results suggested enhanced fracture and fatigue lives of specimens at higher load conditions [32]. An experimental and analytic study of concrete fracture energy was carried out, and mixed mode concrete fracture was examined by comparing the experimental and model results. A brittle diagonal failure was observed [33].

1.1. Research Gap and Goals

Based on the literature review above, the authors of this study observed that although the study of concrete fracture behaviour on notched and unnotched concrete specimens have been undertaken by various researchers, these researchers have considered a combination of a few factors such as compressive strength, water-cement ratio, aggregate type, specimen size (weight), grade of concrete, tensile strength, and temperature. A comprehensive model covering most of these parameters has not been developed yet. Secondly, the usefulness of genetic algorithm (GA)-based software to solve problems of high uncertainty, such as the one involving concrete fracture behaviour, is well known. However, no such GA model exists in the literature studied. Further, only a few researchers have undertaken studies involving both notched and unnotched specimens. Therefore, experimentation on notched and unnotched concrete specimens of RILEM geometry, complemented by a genetic algorithm software-based model of the unnotched specimen considering six key fracture energy parameters, was considered necessary to comprehend concrete fracture behaviour. Accordingly, the study was planned and undertaken.

1.2. Research Significance

Determining fracture energy in the concrete of unnotched specimens is central to this study. This study is significant because it explains the need for extending the experimentation on the notched specimen to the unnotched specimen. Further, the study highlights the relative influence of the various impactful parameters affecting the concrete fracture energy of unnotched specimens. The assessment of this influence for unnotched specimen has been arrived at firstly, by experimental work, secondly by literature models, and finally by a unique Multigene Genetic Programming technique.

2. Materials and Methods

2.1. Notched Specimens

The test specimens were prepared using three grades of concrete, namely M20, M30, and M40. All test specimens were of the RILEM TC-50 [34] recommended geometry of 100 x 100 x 840 mm. Three design mixes of M20, M30, and M40 concrete grades were considered for the investigation. OPC 53-grade cement, M-sand, and coarse aggregates (sizes not exceeding 20 mm) with design water-cement ratios of 0.36, 0.38, and 0.5 for M40, M30, and M20 grades of concrete

were used. In the mixing process, the aggregates were dry mixed for a minute; subsequently, cement and water were added, and the wet concrete was mixed for a further two minutes. On completion of the mixing process, the concrete was poured into the moulds for casting. After de-moulding, the specimens were placed in curing tanks for 28 days before testing. The concrete compressive strengths were tested using the classical methods for the three grades. The design mix details and the experimental compressive strengths are tabulated in Table 1.

Table 1. Details of concrete mix design and experimental compressive strength

Ser No	Constituents	Grade of Concrete (Kg/cubic metre)			Remarks
		M20	M30	M40	
1	OPC 53 Cement	404	408	431	
2	Water	202	155	155	
3	Fine Aggregate	644	638	626	
4	Coarse Aggregate	1065	1176	1173	
5	Admixtures	0	4.08	4.31	1% of cement content
6	W/C ratio	0.500	0.380	0.360	
7	Average Compressive strength in MPa	19.13	28.24	36.77	

The grading curves for fine aggregates and coarse aggregates used in the test specimen casting are shown in Figures 1 and 2.

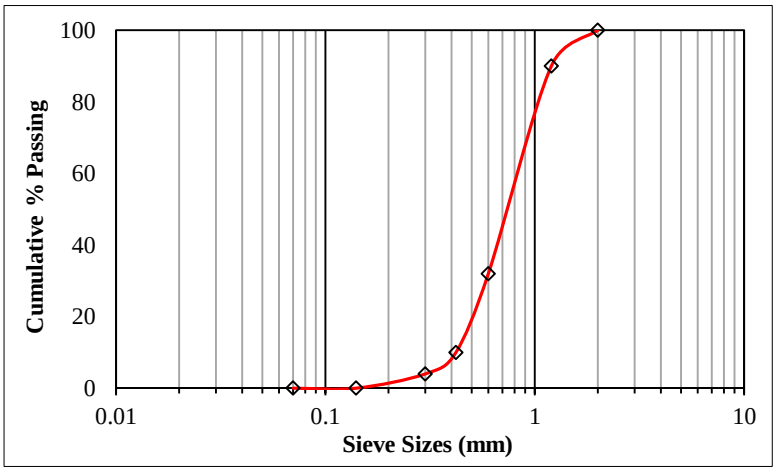

Figure 1. Grading Curve for Fine aggregates used

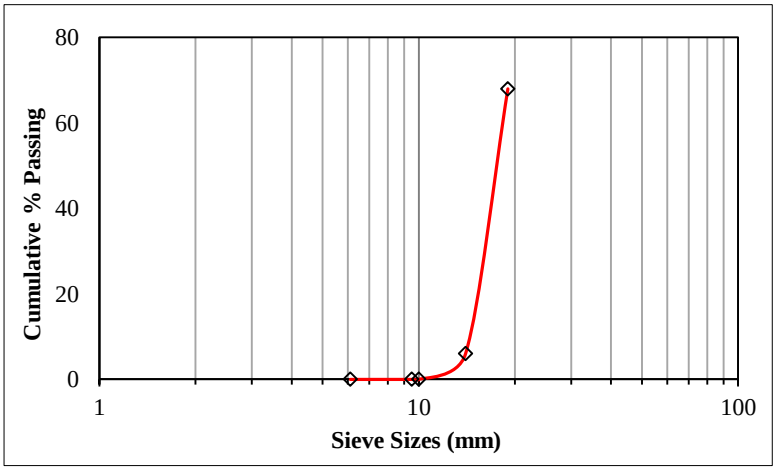

Figure 2. Grading Curve for Coarse aggregates used

To determine different concrete fracture parameters and the related factors of characteristic length and brittleness number, an experimental approach was adopted. In this approach, the classical three-point bending test as recommended by RILEM 50-FMC, was used to test 18 notched specimens of standard size subjected to a concentrated load at the centre. Three different grades of concrete and two notch depths were considered for the investigation. The geometric details of the test specimens are in Table 2.

Table 2. Geometric details of test specimens

Ser. No.	Notched specimen Number	Width b (mm)	Depth d (mm)	Length l (mm)	Effective Span s (mm)	Notch a_o (mm)	A_{lig} (mm²) $(d-a_o)\times b$	Notch-to-depth (Notch ratio)
1	M20-1	100	100	840	800	50	5000	0.5
2	M20-2	100	100	840	800	50	5000	0.5
3	M20-3	100	100	840	800	50	5000	0.5
4	M20-4	100	100	840	800	30	7000	0.3
5	M20-5	100	100	840	800	30	7000	0.3
6	M20-6	100	100	840	800	30	7000	0.3
7	M30-1	100	100	840	800	50	5000	0.5
8	M30-2	100	100	840	800	50	5000	0.5
9	M30-3	100	100	840	800	50	5000	0.5
10	M30-4	100	100	840	800	30	7000	0.3
11	M30-5	100	100	840	800	30	7000	0.3
12	M30-6	100	100	840	800	30	7000	0.3
13	M40-1	100	100	840	800	50	5000	0.5
14	M40-2	100	100	840	800	50	5000	0.5
15	M40-3	100	100	840	800	50	5000	0.5
16	M40-4	100	100	840	800	30	7000	0.3
17	M40-5	100	100	840	800	30	7000	0.3
18	M40-6	100	100	840	800	30	7000	0.3

Two photos of the notched specimen testing and some fractured specimens are as in Figure 3.

Figure 3. Notched specimen under test and some failed specimens

2.2. Unnotched Specimens

The unnotched test specimen were prepared using the same three grades of concrete namely M20, M30 and M40 for the investigation. All test specimens were of the RILEM TC-50 recommended geometry of 100 x 100 x 840 mm. OPC 53 grade cement, M-sand and Coarse aggregates (size not exceeding 20 mm) with design water-cement ratios of 0.36. 0.38 and 0.5 for M40, M30 and M20 grades of concrete were used. The unnotched sample preparation was similar to the sample preparation of the notched specimen. The design mix details and the experimental compressive strengths were the same as for the notched specimen tabulated in Table 1.

An experimental approach combined with the multi-gene genetic programming modelling was adopted to determine different concrete fracture parameters and the characteristic length of the unnotched specimens. In the experimental approach, the classical three-point bending test, as recommended by RILEM TC-50 FMC and Standard JCI, 2003 [35], was used to test nine unnotched specimens of standard size subjected to a concentrated load at the centre. Two criteria dictated the test specimen size. Firstly, the RILEM TC-50 recommendations on the specimen geometry and secondly, the requirement of minimizing the boundary effects on the test results. The specimen's smallest dimension was 100 mm,

in consideration of maintaining the smallest dimension larger than three times the maximum size of the aggregate (20 mm) to minimize the boundary effects. The experimental setup for the conduct of the RILEM test for the unnotched specimen and the failed specimens are in Figure 4.

Figure 4. Unnotched specimen test setup and failed specimens

2.3. Displacement Measurements

The RILEM TC-50 testing for the specimens was conducted using a Universal Testing Machine (UTM) of 1000 KN. Concrete is a known heterogeneous material and the displacements are known to be influenced by the aggregate size. In consideration of the recommendations of Hanson and Kurvits (1965) [36], longer electrical strain gauges, (proportionate to the aggregate size used) were used. Three 350 Ω (size 14 mm × 4.6 mm) electrical strain gauges were used for the displacement measurements, in the regions of uniform strain. Two strain gauges were instrumented at the bottom of the specimen on either side of the specimen centre while the third gauge was positioned on the specimen's depth face at 60 mm from the specimen centre. The hydraulically operated Universal Testing Machine used for controlled loading enabled continuous and without shock loading. A continuous record of load and strain readings were obtained up to fracture failure, using a four-channel data logger connected to a laptop hosting the relevant software.

3. Results and Discussions

3.1. Notched Specimens

The evaluation of the fracture energy of the notched test specimens was carried out by the RILEM 50-FMC recommendations by popular work of fracture method (WFM). This widely accepted test procedure albeit uncomplicated has an inherent limitation of size dependency. Hillerborg et al. (1981) [10] observed that the WFM-based fracture energy values computed in isolation do not adequately represent the brittleness or ductility of the specimens. Therefore, to overcome this limitation, the characteristic length, L_{ch} and the brittleness number β have been initiated into the research realm of concrete fracture behaviour. Also, the G_f and G_F calculations have been in alignment with the recommendations of Bazant et al. (2002) [37] involving a factor of 2.5. The expressions used are below:

$$G_f = \frac{[w_o+\left(m_1*\left(\frac{s}{l}\right)+2m_2\right)*g*\delta_o]}{A_{lig}} \quad (1)$$

$$L_{ch} = \frac{(E*G_F)}{f_t^2} \text{ and } \beta = \frac{l}{L_{ch}} \quad (2)$$

The test results and calculations are in Table 3.

Table 3. Calculated Fracture parameters

Notched specimen number	W_o (N-mm)	δ_o (mm)	F_{max} (N)	G_f (N/m)	G_F (N/m)	Characteristic length L_{ch} (mm)	Brittleness number β
M20-1	55.50	0.42	1200	29.30	73.24	193.08	4.35
M20-2	69.50	0.46	1300	29.95	74.88	219.67	3.82
M20-3	70.00	0.54	1600	30.43	76.07	250.13	3.36
M20-4	52.50	0.54	1600	25.96	64.89	162.19	5.18
M20-5	72.00	0.55	1600	29.47	73.68	184.16	4.56
M20-6	95.50	0.62	1700	30.60	76.49	213.68	3.93
M30-1	94.50	0.61	1700	36.98	92.45	242.29	3.47
M30-2	111.00	0.63	1700	40.66	101.65	265.20	3.17
M30-3	101.00	0.65	1800	40.85	102.13	264.13	3.18
M30-4	113.50	0.66	1800	39.05	97.63	199.70	4.21
M30-5	121.00	0.67	1800	37.42	93.54	203.61	4.13
M30-6	134.50	0.69	1800	38.56	96.41	217.67	3.86
M40-1	112.50	0.7	1800	41.90	104.75	238.79	3.52
M40-2	123.00	0.71	1900	45.78	114.44	255.95	3.28
M40-3	116.50	0.73	2000	42.08	105.19	257.29	3.26
M40-4	153.50	0.77	2100	44.90	112.25	213.09	3.94
M40-5	162.50	0.78	2200	42.68	106.70	224.53	3.74
M40-6	168.50	0.79	2200	43.86	109.65	227.97	3.68

3.1.1. Analysis of Notched Specimen Fracture Parameters

The average fracture energy values from Table 3 for M20, M30 and M40 grades of concrete were experimentally determined as 73.2, 97.3 and 108.83 N/m respectively. The creation of a notch in the concrete specimen has compelled the formation of the fracture zone at a predetermined location of the notch whereas the fracture zone could develop anywhere else in the specimen in case of unnotched specimen. Also, notches are stress raisers due to being points of stress concentrations. Therefore, the creation of a notch in a test specimen is likely to have affected the assessment of the fracture energy G_F in notched specimens. In order to evaluate a realistic concrete fracture energy G_F, it was felt necessary to test unnotched specimens of similar geometry and grades of concrete.

3.2. Unnotched Specimens

The principles of fracture mechanics are equally applicable to the analysis of unnotched specimens. Also, the research work of Bazant & Planas (2019) [38] has highlighted the importance of fracture energy, tensile strength and characteristic length assessments for concrete. They have observed that these three assessments denote the linkage between the crack width and these three parameters. Therefore, these three parameters have been assessed in the present study for unnotched specimens.

The fracture energy experimentation of the unnotched specimen was also carried out following the RILEM 50 – FMC recommendations. As the results were known to be affected by the size dependency and that the brittleness or ductility of the specimens cannot be adequately represented by WFM-based fracture energy results alone, the fracture energy (G_f) results were supplemented with the characteristic length (L_{ch}) value computations. G_f and Lch were calculated based on Equations 1 and 2 mentioned earlier. The fracture energy factor 2.5 of Bazant et al. (2002) [37] was adopted for G_f to G_F conversion. The fracture energy and the characteristics length calculations of the specimen have been tabulated in Table 4.

Table 4. Fracture energy and characteristic length calculations

Ser. No.	Unnotched specimen Number	Water cement ratio (w/c)	δ_o (mm)	F_{max} N	w_o (N-mm)	G_F (N/M)	Characteristic length L_{ch} (mm)
1	M20-1U	0.5	0.49	2400	221.75	82.55	210.67
2	M20-2U	0.5	0.49	2400	225.25	84.29	215.11
3	M20-3U	0.5	0.52	2500	222.25	85.24	200.48
4	M30-1U	0.38	0.62	2600	319.5	113.90	303.34
5	M30-2U	0.38	0.62	2500	333.75	117.12	337.35
6	M30-3U	0.38	0.63	2600	332.5	117.86	313.88
7	M40-1U	0.36	0.69	2800	430.5	145.79	386.56
8	M40-2U	0.36	0.70	2900	425.25	146.27	361.55
9	M40-3U	0.36	0.70	2900	422.25	144.13	382.16

All nine load-deflection relationships have been plotted and only three load-deformation curves for M20, M30 and M40 plotted for G_f estimations have not been reported for brevity. The plotted curves are shown in Figure 5.

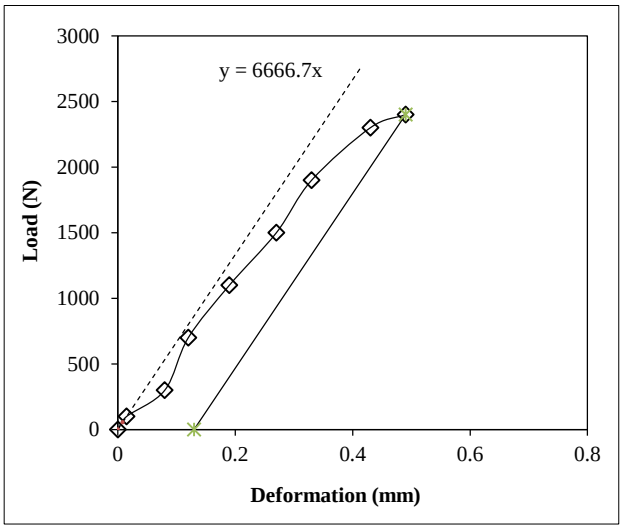

(a) M20 Load – deformation curve

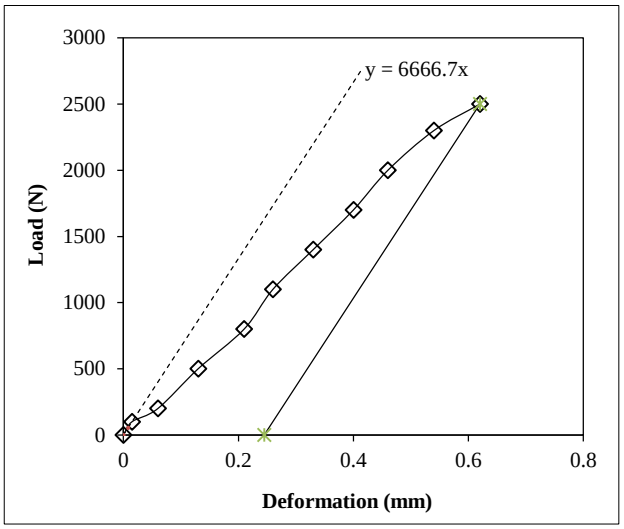

(b) M30 Load – deformation curve

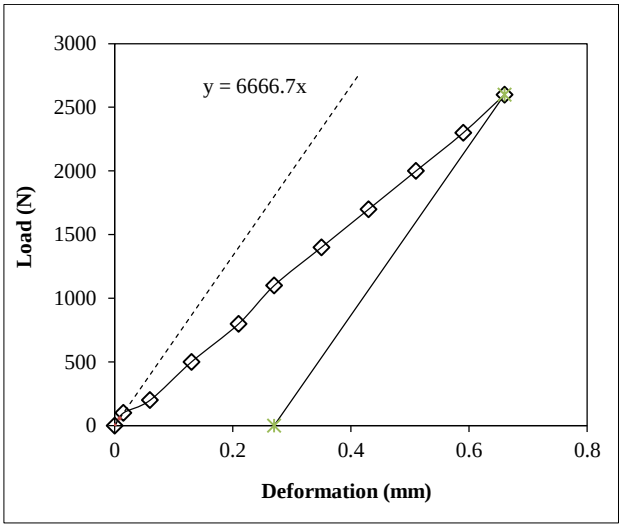

(c) M40 Load – deformation curve

Figure 5. Load-deformation curves for M20, M30 and M40

3.2.1. Analysis of the Fracture Energy Values of Unnotched Specimens vis-à-vis Notched Specimens

The average fracture energy values from Table 4 for M20, M30 and M40 grades of concrete were experimentally determined as 84.02, 116.3 and 145.4 N/m respectively. The corresponding average fracture energy values for notched specimens from Table 3 for M20, M30 and M40 grades of concrete were 73.2, 97.3 and 108.83 N/m respectively. There was a noticeable increment in the assessed fracture energy values in unnotched specimen in comparison to the corresponding values of the notched specimen and this was attributable to the creation of a stress concentration areas around the notch in notched specimens. A more definitive evaluation of the percentage increment could emerge from a larger experimental data set.

3.2.2. Fracture Energy and Characteristic Length vs. Various Grades of Concrete of Unnotched Specimens

The variations in the average fracture energy and the characteristic length of the unnotched specimens with respect to the concrete grades have been depicted in Figure 6. Higher grades of concrete have exhibited higher fracture energy reflective of their tendency to be brittle with increasing compressive strengths. As already reported by Darwin et al. (2001) [39], an increase in compressive strength of concrete increased the stored energy at the peak load without altering the energy dissipation and thus, led to enhanced brittleness at higher compressive strengths. A direct proportionality relationship between G_F and L_{ch} as already reported in the literature by Rosselló et al. (2006) [40], was confirmed in these test results.

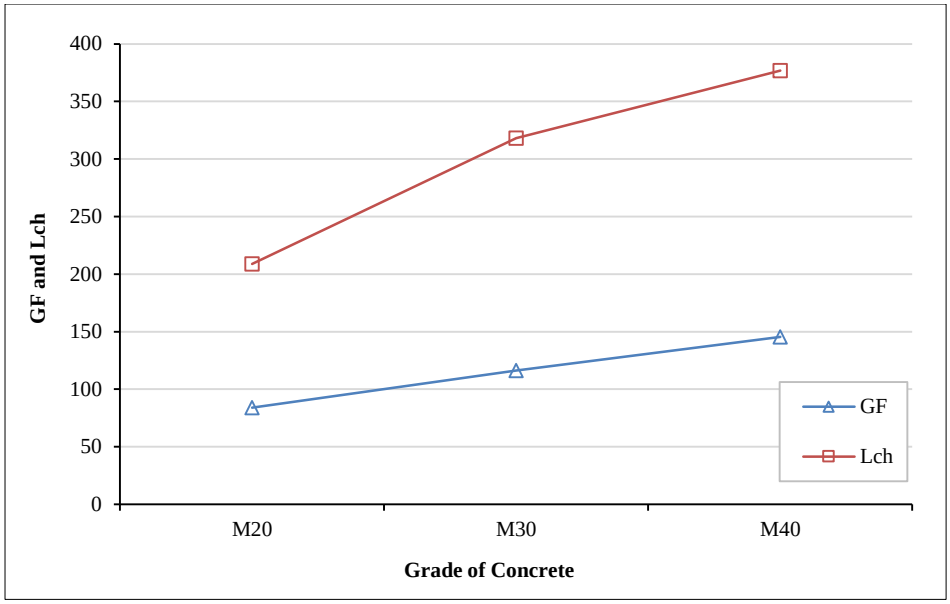

Figure 6. Variation of G_F and L_{ch} with concrete grades

3.2.3. Fracture Energy vs. Water-Cement Ratio of Concrete of Unnotched Specimens

The water-cement ratio has been of significant interest to researchers as the water-cement ratio has a pronounced influence on the porosity of ITZ of concrete and therefore, the effect of the water-cement ratio on the fracture energy was examined. The test results confirmed the inverse relationship between the fracture energy and the water-cement ratio as suggested by Ostergaard et al. (2004) [17] in the literature. The details of the fracture energy of unnotched specimen and the water-cement ratio have been exhibited in Figure 7.

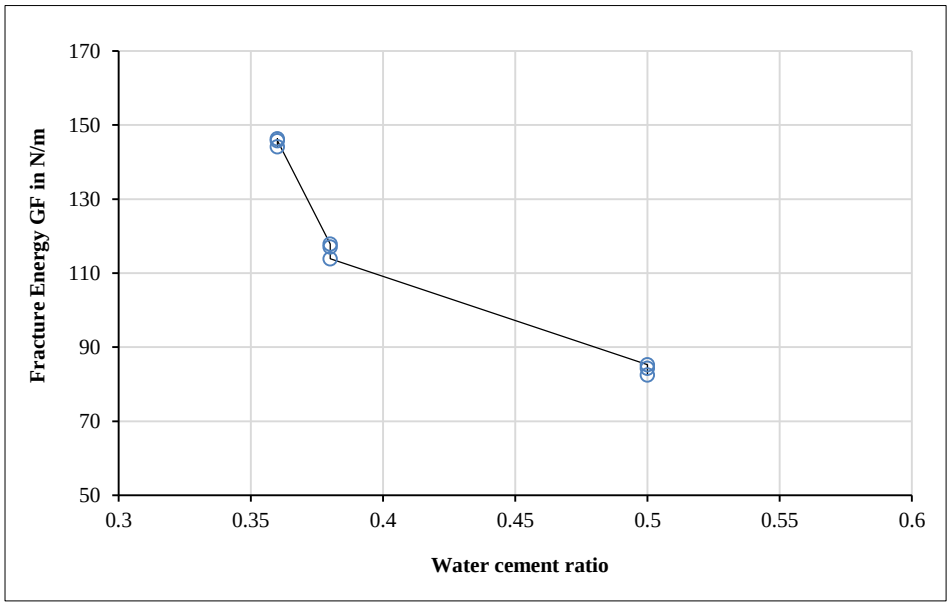

Figure 7. Fracture energy vs. water-cement ratio

3.2.4. Tensile Strength Computations of Specimens by Various Models

The tensile strength can quantify the peak load behaviour. A frequently employed test procedure for unnotched specimens has been the flexural tensile strength determination in a three-point bend test [10]. Also, as the direct tensile strength test of concrete is experimentally complicated to conduct for assessment of fracture behaviour, the flexural tensile strength test of concrete was adopted. The modulus of rupture obtained by performing the fracture test on concrete gave the theoretical maximum tensile stress under bending on the concrete specimens. The computed values of the tensile strength from the various models have been displayed in Table 5.

Table 5. Tensile strength calculations by various models

Ser No	Specimen Number	F_{max} (N)	Experimental Modulus of rupture (fr) MPa	IS 456: (2000) [41] (fr) MPa	Hilsdorf and FIB code (2010) [42] (fctm) MPa	ACI 318-14 [43] (ft) MPa	ACI 363 – (1993) [44] (ft) MPa	Philips [45] (ft) MPa
1	M20-1	2400	2.88	3.13	2.21	2.91	2.34	1.97
2	M20-2	2400	2.88	3.13	2.21	2.91	2.34	1.97
3	M20-3	2500	3	3.13	2.21	2.91	2.34	1.97
4	M30-1	2600	3.12	3.83	2.9	3.56	2.95	2.39
5	M30-2	2500	3	3.83	2.9	3.56	2.95	2.39
6	M30-3	2600	3.12	3.83	2.9	3.56	2.95	2.39
7	M40-1	2800	3.36	4.42	3.51	4.11	3.42	2.73
8	M40-2	2900	3.48	4.42	3.51	4.11	3.42	2.73
9	M40-3	2900	3.36	4.42	3.51	4.11	3.42	2.73

3.2.5. Fracture Energy Calculations Based on the Existing Models and This Study

Fracture energy can also be predicted based on aggregate size, compressive strength and water-to-cement ratio as suggested in the models of Hilsdorf & Brahmeshuber (1991) [14], Philips & Binsheng (1993) [45], Wittman et al. (1987) [12], Standard JCI (2003) [35], Comite Euro-International du Beton (CEB-2010) [42], and Mari et. al. (2015) [21]. These study models are mentioned below:

$$G_F = a_d * (f_{cm})^{0.7} \quad (3)$$

$$G_F = 43.2 + 1.13 * f_c \quad (4)$$

$$G_F = 30.5 + 6.64 * f_t^{(2)} \quad (5)$$

$$G_F = [0.97 * (f_c) + 41.8] \quad (6)$$

$$G_F = \frac{0.75*[w_o+\left(m_1*\left(\frac{s}{l}\right)+2m_2\right)*g*\delta_o]}{A_{lig}} \quad (7)$$

$$G_F = 73 * f_c^{0.18} \quad (8)$$

$$G_F = 0.028 * (D_{max})^{0.32} * (f_{cm})^{0.18} \quad (9)$$

where a_d is a coefficient dependent on maximum aggregate size (a_d=7 for max aggregate size of 20 mm), f_{cm} is $(f_{ck} + 8)$ in MPa, f_c is the experimental compressive strength in MPa, f_t is the tensile strength of specimen, w_0 is the area under the load-deformation curve, m_1 is the weight of the specimen in kg, m_2 is the weight of external attachments to the test setup in kg, s is the effective span of specimen in mm, l is the length of specimen in mm, g is the acceleration due to gravity in m/sec^2, ∂_0 is the max displacement at failure in mm and A_{lig} is the area of the specimen fracture surface. The calculated fracture energy of concrete determined based on various models and as per experimentation of this study have been mentioned in Table 6.

Table 6. Fracture energy computations by various models and this study

Ser No	Specimen Number	fc (MPa)	Hilsdorf (1991) G_F in N/m	Philips 1 (1993)G_F (N/m)	Philips 2 (1993) G_F (N/m)	Wittman (2002) G_F (N/m)	JCI-S-001-(2003)	FIB (2010) G_F (N/m)	Mari (2015) G_F (N/m)	Experiment G_F (N/m)
1	M20	19.14	72.13	64.83	56.27	60.37	63.02	124.19	124.23	84.03
2	M30	28.24	89.32	75.11	68.43	69.19	87.22	133.19	133.24	116.29
3	M40	36.77	105.19	84.75	79.99	77.47	119.05	139.67	139.73	145.4

Among the seven models studied, six models used compressive strength, tensile strength, and maximum aggregate size as the influencing parameters for the fracture energy calculations. The Japanese JCI code has adopted a modified expression of the original Hillerborg model for the fracture energy computations. Hilsdorf, Philips I and II, Wittman, and JCI models provide fairly conservative fracture energy estimates. The JCI code has modified the original Hillerborg fracture energy expression by using a factor of 0.75. Therefore, the experimental values of this study and the JCI code values are related by this factor of 0.75. FIB 2010 and Mari models yielded nearly identical fracture energy values for the three grades of concrete and suggested that the fracture energy values were independent of the concrete grades.

Because the fracture energy computations are complex, the experimental and literature model assessments must be validated against the regression analysis model. Therefore, this investigation has employed the experimental data of the study as well as the literature data to develop a multi-gene genetic model for concrete fracture energy determination.

3.2.6. Summary of Results

Traditionally, research on the concrete fracture behaviour has revolved around the notched specimen testing for fracture parameter determination. However, as this study has shown, for a realistic estimation of concrete fracture behaviour, both notched and unnotched specimens have to be tested. This study confirmed the direct relationship between (the fracture energy and the characteristic length) vs. (the grade of concrete) as well as the inverse relationship between (the fracture energy) vs. (the water-cement ratio) as reported in literature. Further, the fracture energy computations by various researchers were based on a few select parameters only. This study has explored the fracture energy of unnotched concrete specimens considering six key parameters by the genetic algorithm-based software as below.

3.3. Multi-Gene Genetic Programming (MGGP)

Multi-Gene Genetic Programming, a variant of Genetic Programming, which adopts a software-based search technique involving mathematical expressions, decision trees, polynomial constructs, logical expressions etc., was employed for model development for the study. First, the chromosomes were generated randomly for each individual in the population. Then the fitness of each of these chromosomes was evaluated based on a fitness function.

$$f = \sum_{j=1}^{N} (X_j - Y_j) \quad (10)$$

where X_j was the value returned by the chromosome for the fitness case j and Y_j was the expected value for the fitness case j. RMSE was used as a fitness function to develop the MGGP model.

In this MGGP algorithm, several potential models were evolved at random and, each such developed model was trained and tested using the training and testing data respectively. The fitness of each model was determined by minimizing the root-mean-square error (RMS) between the predicted and actual value of the output variable (G_F). Multigene-based chromosomes of unequal lengths consisting of variables and mathematical operators were used. The individuals in the process were subjected to modifications, which were repeated until the desired solution was achieved. The chromosomes in the study were either unigenic (single gene) or multigenic with equal or unequal program lengths consisting of variables and mathematical operators (function set). The mathematical operators used were arithmetic (+; -; *; /) and functions (log 10 and exponential).

GeneXpro Tools 5.0 was used for modelling the gene expression programming in this study. It worked with a population of models selected according to their respective fitness. The selected models were reproduced by introducing genetic variations using one or more genetic operators like mutation or recombination. Repetition of this process till the desired solution was achieved, provided an improved and the best fit model for the data set.

3.3.1. Methodology of MGGP Model Building

This research has proposed an MGGP prediction model for concrete fracture energy using the experimental and literature data as inputs. The concrete fracture energy profile was generated with accuracy using the developed model for the complex data set. Figure 8 represents the methodology flow to provide a robust concrete fracture energy prediction model starting from the data compiled. This step was followed by data pre-processing which included data cleaning and removal of the outliers to offer input parameters of quality for the model formulation. The next step was to build and optimize the model by repetitively training and optimizing with the trained algorithm. The model accuracy and performance were determined by sensitivity and error analysis and covered MAE, MAPE, RMSE and R^2 computations. Whenever the desired accuracy was not attained, the model was retrained to till acceptable accuracy of prediction was achieved. Finally, the model parameters and the results were saved and reported.

3.3.2. Choice of Model Parameters

After a detailed literature study of various models from Hillerborg (1983) [46], Hillerborg (1985) [47], CEB-FIP model code (1990) [48], Bazant et al. (1991) [49], Elices et al. (1992) [50], Darwin et al. (2001) [39], Strauss et al. (2002) [51], Standard JCI (2003) [35], Martin et al. (2007) [52], Comite Euro-International du Beton (CEB-2010) [42], Khatieb (2016) [53], Beygi et al. (2016) [54], Khalilpour et al. (2019) [24] and Akram (2021) [55], six independent variables affecting the concrete fracture energy were chosen for modelling. They are grade of concrete (G), water-cement ratio (w/c), maximum displacement at failure (∂_0), maximum load at fracture (F_{max}), curing period in days (C) and the tensile strength of concrete (f_t).

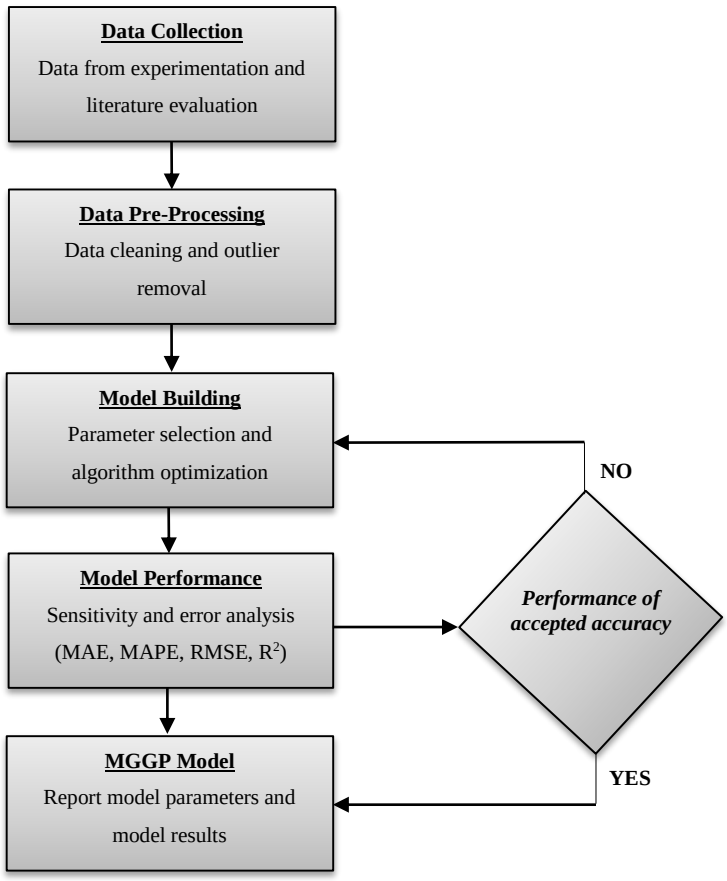

Figure 8. Methodology of MGGP model developed

3.3.3. Development of Model

The model developed in this study has designated the concrete fracture energy as the output and the six independent parameters selected above and shown in Equation 11 as inputs:

$$G_F = f\ (G, w/c, \partial_0, F_{max}, C, f_t) \quad (11)$$

Four basic arithmetic operators (+; -; *; /) and two basic mathematical functions (log 10 and exp.) were used as a function set in the model development. Multi-genic programming with four genes and addition as the linking function were used. A large number of generations (599) were tested. The functional set and operational parameters used in the MGGP modelling during this study have been listed in Table 7.

Table 7. Functional set and Operational parameters

Description of Parameter	Parameter setting
Data	
Independent Variables	06
Training Records	21
Validation Records	10
Program size	40
Function Set	+, -, *, /, exp, log 10
Settings	
Number of Chromosomes	30
Number of genes	4
Head Size	8
Tail size	9
Gene size	26
Linking function	Addition
Fitness function	RMSE
Iteration – R^2 threshold	1
Constant per gene	7
Data type	Integer

The overall 31 datasets are randomly distributed as 70% training and the rest 30% as testing data. The datasets did not need normalizations in the analysis, as the modelling was carried out by the fitness function which generates an expression to calculate concrete fracture energy from the depending parameters. These parameters, whether dimensional or non-dimensional can be used directly in their usual form, i.e., the one used during the model generation to calculate the concrete fracture energy G_F.

3.3.4. Training and Validation of MGGP Models

Table 8 illustrates the statistics for the training and validation of the model with the values of the various errors generated in the model's prediction. The training dataset has a high R^2 value while the validation dataset has a relatively lower R^2 value. This probably is attributable to the limited dataset of this research work.

Table 8. Statistics for Training and Validation

Statistics	Training	Validation
R-square	0.921273577	0.742463807
Correlation Coefficient	0.95982997298283	0.86166339545024
Root Mean Squared Error	14.5267504483885	22.871845
Mean Absolute Error	10.6219601881548	15.58426511
Best Fitness	64.4049766449224	41.891335940425

Figure 9 shows the MGGP tree of the model for predicting the concrete fracture energy G_F, which has been illustrated in a simplified analytical formulation as:

$$G_F = \left(e^{4.10\frac{Fmax}{G}}\right) * \left(e^{(8\delta_0 - f_t)}\right) + \frac{c}{e^{(1.92+w/c)*(0.33-9.77\delta_0)}} + \frac{7.46}{w/c}(1.34 + f_t) + (\delta_0 * (Fmax + G)) + 3.05 \quad (12)$$

Sub – ET 1

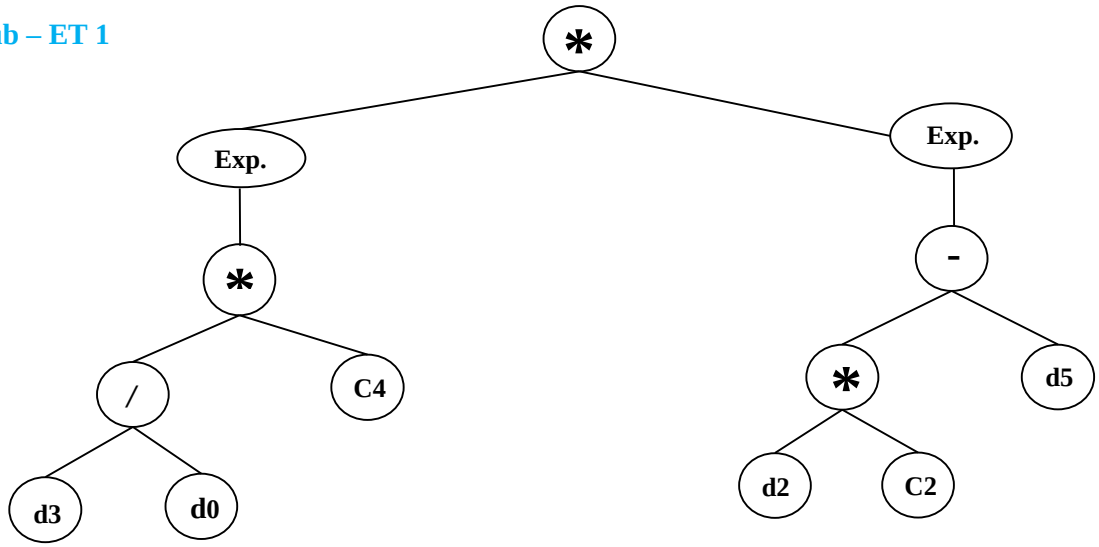

Sub – ET 2

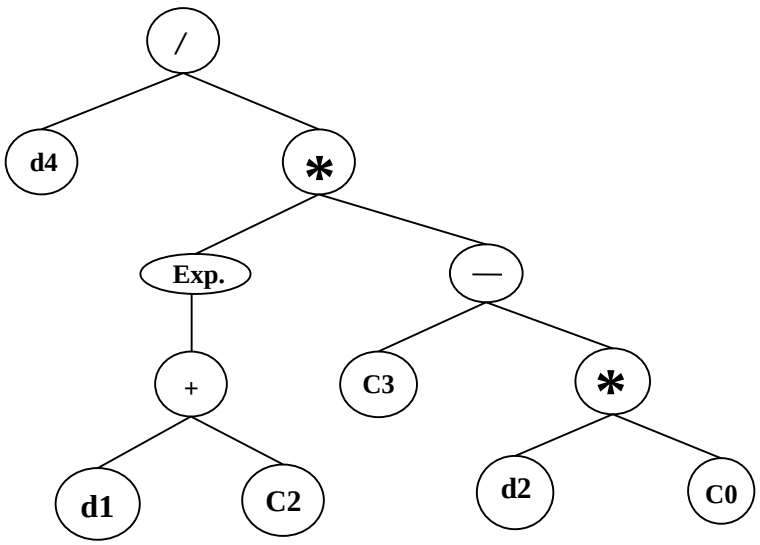

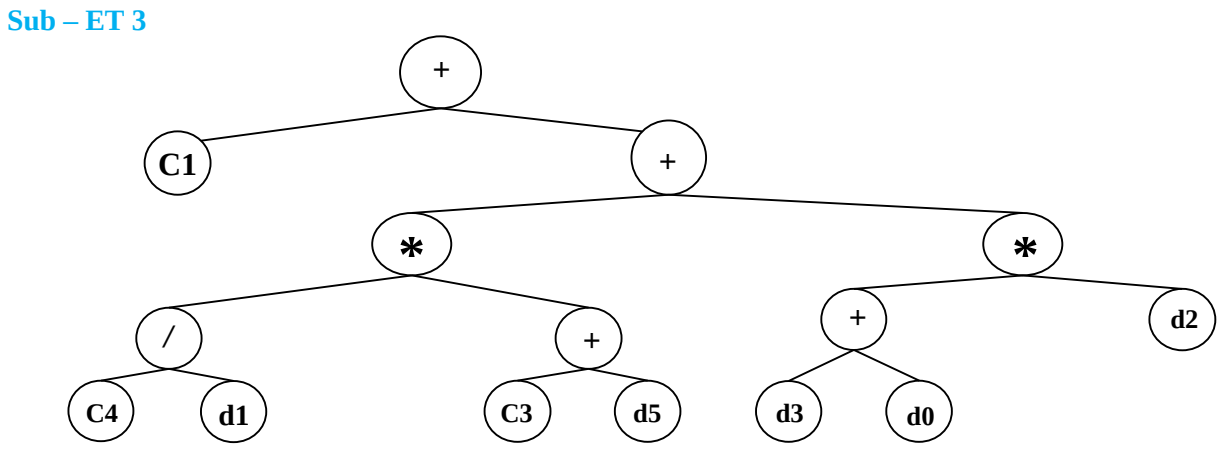

Figure 9. MGGP Tree for Fracture energy G_F model

3.3.5. Sensitivity Analysis

The sensitivity of the assumed parameters, for the new MGGP model was essential to determine the influence and importance of each. The sensitivity percentage for the six parameters was found using the following expressions:

$$N_i = f_{max}(x_i) - f_{min}(x_i) \quad (13)$$

$$S_i = \left(\frac{N_i}{\sum_{j=1}^{n} N_j}\right) * 100 \quad (14)$$

where $f_{max}(x_i)$ and $f_{min}(x_i)$ were the respective values of maximum and minimum predicted output over the i^{th} input domain where the other variables were equal to their mean values. S_i represents the sensitivity percentage presented in Table 9 for all the chosen parameters.

Table 9. Sensitivity of the parameters

Parameter	G	w/c	∂_0	F_{max}	C	f_t
Sensitivity in %	4.50	19.78	32.73	23.12	1.78	18.08

It was observed from Table 9 that the maximum displacement at failure and the maximum load at failure have the highest effects on the concrete fracture energy with 32.73% and 23.12% respectively; followed by the water-cement ratio and the tensile strength with 19.78% and 18.08% respectively. The grade of concrete and the curing period appear to have the least influence with 4.5% and 1.78% respectively. To observe the effect of each of these parameters on the fracture energy, a more comprehensive analysis was carried out for the expression of the fracture energy by MGGP in Equation 12. For the analysis, the values for each parameter were fixed as the mean values from the datasets in the study. To observe the effect of an individual parameter, the values of that parameter were varied between its maximum and minimum values as per the datasets, keeping the values of the other parameters as their respective mean values.

The graphical representation of this technique for various parameters has been illustrated in Figure 10. It was observed that the fracture energy was directly proportional to the maximum displacement at failure, maximum load at failure, the tensile strength and the grade of concrete. Also, the fracture energy was inversely proportional to the water-cement ratio. The fracture energy and the curing period graph suggested a weak relationship within the framework of the dataset and hence, need further research exploration.

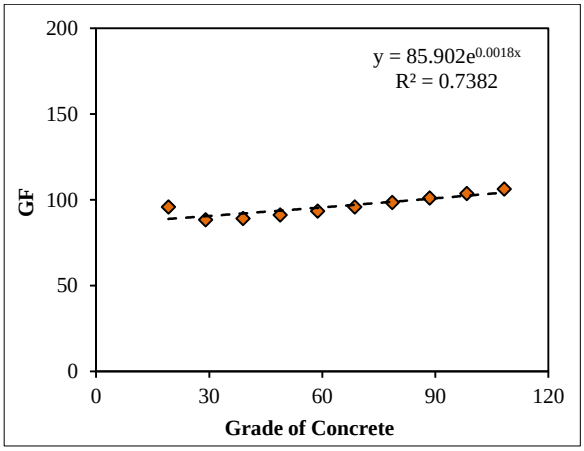

(a) Graph of GF vs. concrete grade

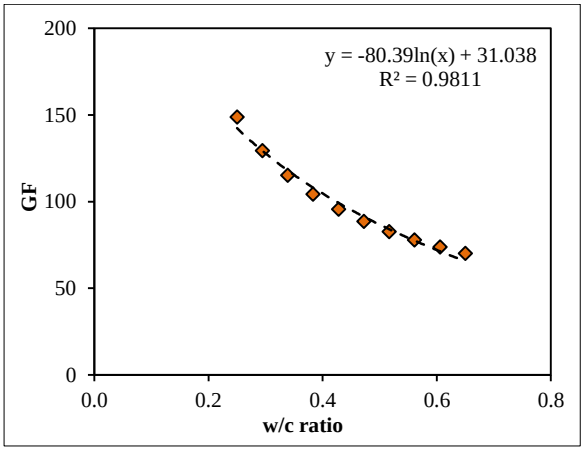

(b) Graph of GF vs. w/c ration

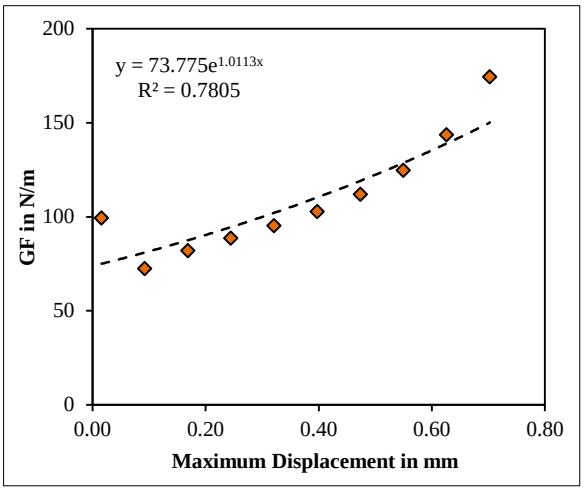

(c) Graph of GF vs. max displacement

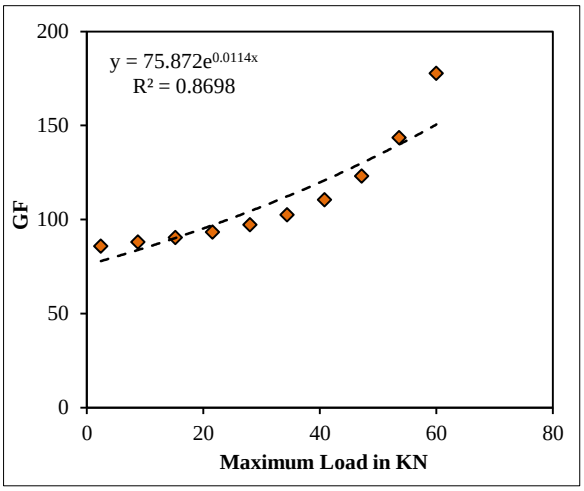

(d) Graph of GF vs. max load at fracture

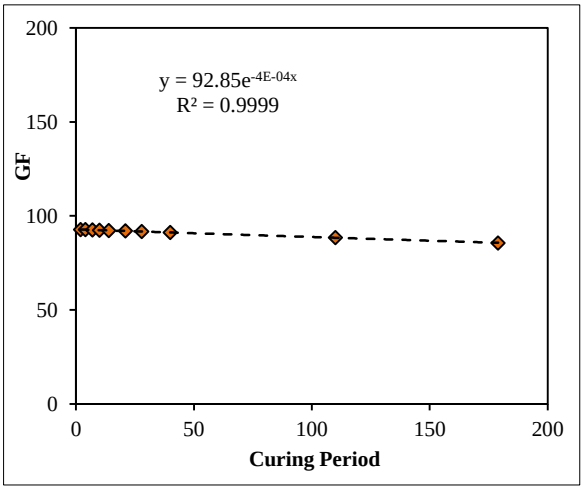

(e) Graph of GF vs. curing period

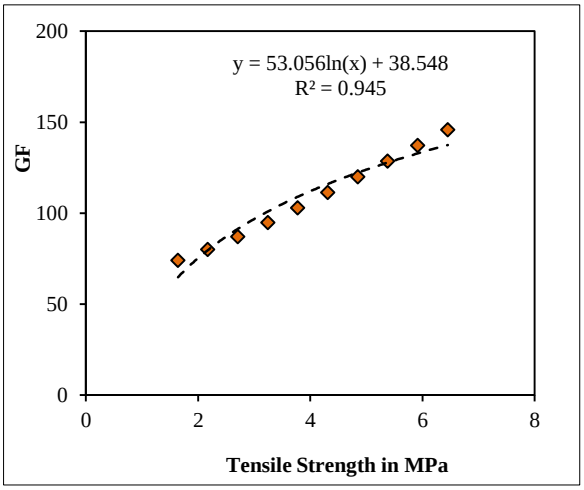

(f) Graph of GF vs. tensile strength

Figure 10. Fracture energy (G_F) graphs with independent variables

The predicted fracture energy in relation to the actual fracture energy for the study is depicted in Figure 11. From Figure 11, with a R^2 value of 0.87, the efficacy of the model is well established.

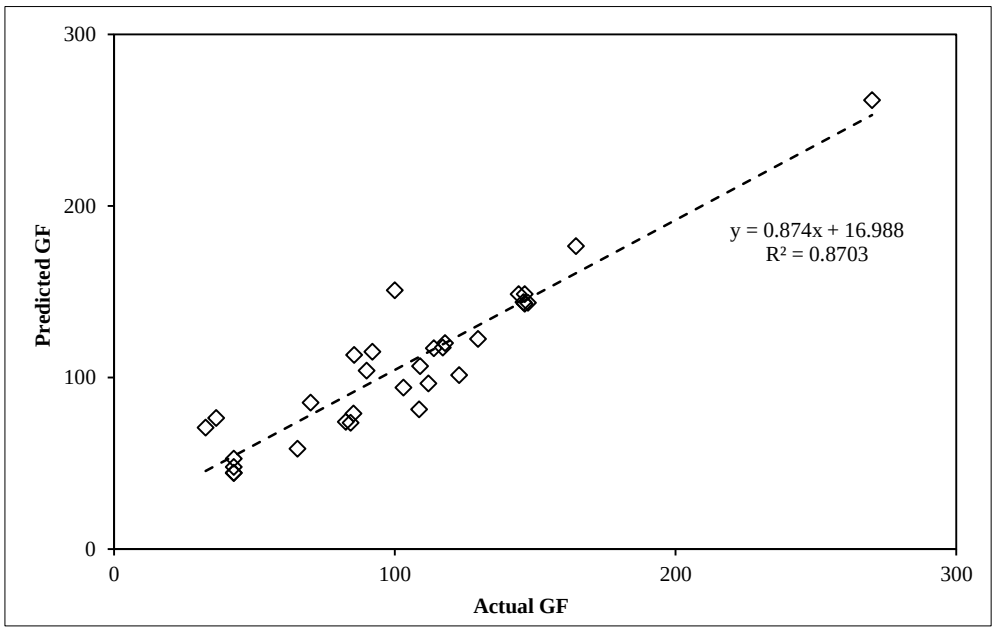

Figure 11. Actual vs. Predicted G_F graph

To test the strengths and weaknesses of the model, error analysis in terms of the mean absolute error (MAE), the mean absolute percentage error (MAPE), the root mean squared error (RMSE), and R^2 values have been computed and tabulated as in Table 10.

Table 10. Error Analysis

Mean Error	10.2
Standard Deviation	31.75
R^2	0.87
MAE	12.43
RMSE	17.68
MAPE	18.02

The developed model (Equation 12) has exhibited a high coefficient of determination (R^2) value and good model accuracy as reflected by the MAE, RMSE, and MAPE percentage values. Overall, the model developed can be considered robust and consistent for similar data sets and variables.

4. Conclusion

The fracture energy values of the unnotched specimen were found to be noticeably higher than the fracture energy values of the notched specimen. This was ascribable to the fact that notches are areas of stress concentration and lead to lower fracture energy estimations than the actual energy values. The experimental results substantiated the conclusion of Darwin et al. (2001) that increasing compressive strength among higher grades of concrete specimens, indicative of increasing brittleness. A possible explanation for this direct relation was the inability of concrete to dissipate higher energy at peak loads of fracture for increasing grades of concrete. An observation of the fracture failure mode of the unnotched specimens suggested the fracture failure occurrence within the specimen central region and hence, was similar to the notched specimen failure modes. The sensitivity analysis of the MGGP model highlighted that the maximum displacement at failure, maximum load at failure, water-cement ratio, and tensile strength of specimens have a pronounced impact on the fracture behaviour. The sensitivity analysis also revealed, within the framework of the experimental and literature datasets used for the model, the lesser influence of the curing period and the concrete grade on the fracture behaviour. The unique MGGP model developed with six influential parameters can be considered robust and accurate based on the error analysis and the R^2 values and is a significant contributor to the new knowledge in the domain when based on the experimental results of notched and unnotched specimen concrete fracture energy determination.

The limitations of the study were that a relatively small sample size for specimens was utilized, and a single cross section of the specimens was employed in the study. The study holds much promise and should be extended to cover varying maximum aggregate size, different specimen cross sections, and also SCM-based concrete and fibre-reinforced concrete in the future.

5. Declarations

5.1. Author Contributions

Conceptualization, S.M.R.; methodology, B.M.; software, S.M.R.; validation, S.M.R., and B.M.; formal analysis, S.M.R.; investigation, S.M.R.; resources, S.M.R., and B.M.; data curation, B.M.; writing—original draft preparation, S.M.R.; writing—review and editing, B.M.; supervision, B.M. All authors have read and agreed to the published version of the manuscript.

5.2. Data Availability Statement

The data presented in this study are available in the article.

5.3. Funding

The authors received no financial support for the research, authorship, and/or publication of this article.

5.4. Acknowledgements

The authors acknowledge the support from the CHRIST (Deemed to be University), Bangalore, in this study. The authors also thank Lt Col Manu Chhabra, GE (I) R&D, DRDO, Bangalore East and his team for their assistance in the casting of specimens and experimentation.

5.5. Conflicts of Interest

The authors declare no conflict of interest.

6. References

[1] Karihaloo, B. L., Abdalla, H. M., & Xiao, Q. Z. (2003). Size effect in concrete beams. Engineering Fracture Mechanics, 70(7–8), 979–993. doi:10.1016/S0013-7944(02)00161-3.

[2] Abdalla, H. M., & Karihaloo, B. L. (2004). A method for constructing the bilinear tension softening diagram of concrete corresponding to its true fracture energy. Magazine of Concrete Research, 56(10), 597–604. doi:10.1680/macr.2004.56.10.597.

[3] Cedolin, L., & Cusatis, G. (2008). Identification of concrete fracture parameters through size effect experiments. Cement and Concrete Composites, 30(9), 788–797. doi:10.1016/j.cemconcomp.2008.05.007.

[4] Raghu Prasad, B. K. (2009). Experimental evaluation of fracture properties of concrete. Interim progress report under collaborative research project between BARC and Indian Institute of Science, Bangalore, India.

[5] Muralidhara, S., Prasad, B. K. R., Eskandari, H., & Karihaloo, B. L. (2010). Fracture process zone size and true fracture energy of concrete using acoustic emission. Construction and Building Materials, 24(4), 479–486. doi:10.1016/j.conbuildmat.2009.10.014.

[6] Skaryński, L., & Tejchman, J. (2010). Calculations of fracture process zones on meso-scale in notched concrete beams subjected to three-point bending. European Journal of Mechanics, A/Solids, 29(4), 746–760. doi:10.1016/j.euromechsol.2010.02.008.

[7] Ince, R., & Cetin, S. Y. (2019). Effect of grading type of aggregate on fracture parameters of concrete. Magazine of Concrete Research, 71(16), 860–868. doi:10.1680/jmacr.18.00095.

[8] Shah, S.P. & Ouyang, C. (1992). Measurement and Modeling of Fracture Processes in Concrete. Materials Science of Concrete. Materials Science of Concrete III, III(I), 243–270, Jan Skalny, United States.

[9] Mehta, P. K. (1986). Concrete. Structure, properties and materials. Prentice Hall, Hoboken, United States.

[10] Hillerborg, A., & Petersson, P. E. (1981). Fracture mechanical calculations, test methods and results for concrete and similar materials. Advances in Fracture Research, 4, 1515-1522.

[11] Mindess, S. (1984). The effect of specimen size on the fracture energy of concrete. Cement and Concrete Research, 14(3), 431–436. doi:10.1016/0008-8846(84)90062-0.

[12] Wittmann, F. H., Roelfstra, P. E., Mihashi, H., Huang, Y. Y., Zhang, X. H., & Nomura, N. (1987). Influence of age of loading, water-cement ratio and rate of loading on fracture energy of concrete. Materials and Structures, 20(2), 103–110. doi:10.1007/BF02472745.

[13] Bazant, Z. P. (2003). Fracture Mechanics of Concrete Structures: Proceedings of the First International Conference on Fracture Mechanics of Concrete Structures (FraMCoS1, 1-5 June 1992,), Colorado, United States, CRC Press, London, United Kingdom. doi:10.1201/9781482286847.

[14] Hilsdorf, H. K., & Brameshuber, W. (1991). Code-type formulation of fracture mechanics concepts for concrete. International Journal of Fracture, 51(1), 61–72. doi:10.1007/BF00020853.

[15] Bazzant, Z. P., & Planas, J. (1998). Fracture and size effect in concrete and other quasibrittle materials. CRC Press, Boca Raton, United States.

[16] Planas, J., Elices, M., Guinea, G. V., Gómez, F. J., Cendón, D. A., & Arbilla, I. (2003). Generalizations and specializations of cohesive crack models. Engineering Fracture Mechanics, 70(14), 1759–1776. doi:10.1016/s0013-7944(03)00123-1.

[17] Østergaard, L., Lange, D., & Stang, H. (2004). Early-age stress-crack opening relationships for high performance concrete. Cement and Concrete Composites, 26(5), 563–572. doi:10.1016/S0958-9465(03)00074-X.

[18] Peterson, P. E. (1980). Fracture energy of concrete: Method of determination. Cement and Concrete Research, 10(1), 79–89. doi:10.1016/0008-8846(80)90054-X.

[19] Hoover, C. G., P. Bažant, Z., Vorel, J., Wendner, R., & Hubler, M. H. (2013). Comprehensive concrete fracture tests: Description and results. Engineering Fracture Mechanics, 114, 92–103. doi:10.1016/j.engfracmech.2013.08.007.

[20] Hoover, C. G., & Bažant, Z. Z. (2013). Comprehensive concrete fracture tests: Size effects of Types 1 & 2, crack length effect and postpeak. Engineering Fracture Mechanics, 110(281), 281–289. doi:10.1016/j.engfracmech.2013.08.008.

[21] Marí, A., Bairán, J., Cladera, A., Oller, E., & Ribas, C. (2015). Shear-flexural strength mechanical model for the design and assessment of reinforced concrete beams. Structure and Infrastructure Engineering, 11(11), 1399–1419. doi:10.1080/15732479.2014.964735.

[22] Herbrand, M., Stark, A., & Hegger, J. (2019). Size effect in unnotched concrete specimens in bending: An analytical approach. Structural Concrete, 20(2), 660–669. doi:10.1002/suco.201800136.

[23] Chen, Y., Han, X., Hu, X., Wang, B., & Zhu, W. (2019). A strength criterion for size effect on quasi-brittle fracture with and without notch. Proceedings of the 10th International Conference on Fracture Mechanics of Concrete and Concrete Structures. doi:10.21012/fc10.229373.

[24] Khalilpour, S., BaniAsad, E., & Dehestani, M. (2019). A review on concrete fracture energy and effective parameters. Cement and Concrete Research, 120, 294–321. doi:10.1016/j.cemconres.2019.03.013.

[25] Wang, X., Saifullah, H. A., Nishikawa, H., & Nakarai, K. (2020). Effect of water–cement ratio, aggregate type, and curing temperature on the fracture energy of concrete. Construction and Building Materials, 259, 119646. doi:10.1016/j.conbuildmat.2020.119646.

[26] Mobasher, B. (2022). M&S Highlight: Hillerborg (1985), the theoretical basis of a method to determine the fracture energy GF of concrete. Materials and Structures, 55(2), 1–3. doi:10.1617/s11527-021-01859-8.

[27] Albayrak, G., & Albayrak, U. (2016). Investigation of Ready Mixed Concrete Transportation Problem Using Linear Programming and Genetic Algorithm. Civil Engineering Journal, 2(10), 491–496. doi:10.28991/cej-2016-00000052.

[28] Wu, K., Chen, B., & Yao, W. (2000). Study on the AE characteristics of fracture process of mortar, concrete and steel-fiber-reinforced concrete beams. Cement and Concrete Research, 30(9), 1495-1500. doi:10.1016/S0008-8846(00)00358-6

[29] Ince, R., & Fenerli, C. (2022). Determination of tensile strength of cementitious composites using fracture parameters of two-parameter model for concrete fracture. Construction and Building Materials, 344, 128222. doi:10.1016/j.conbuildmat.2022.128222.

[30] Guan, J. F., Song, Z. K., Yao, X. H., Chen, S. S., Yuan, P., & Liu, Z. P. (2020). Determination of fracture toughness of concrete and rock using unnotched specimens. Gongcheng Lixue/Engineering Mechanics, 37(3), 36–45. doi:10.6052/j.issn.1000-4750.2019.03.0082. (In Chinese).

[31] Ince, R. (2021). Utilization of splitting strips in fracture mechanics tests of quasi-brittle materials. Archive of Applied Mechanics, 91(6), 2661–2679. doi:10.1007/s00419-021-01913-5.

[32] Stephen, S. J., & Gettu, R. (2020). Fatigue fracture of fibre reinforced concrete in flexure. Materials and Structures/Materiaux et Constructions, 53(3), 1–11. doi:10.1617/s11527-020-01488-7.

[33] Daneshyar, A., Ghaemian, M., & Du, C. (2022). A fracture energy–based viscoelastic–viscoplastic–anisotropic damage model for rate-dependent cracking of concrete. International Journal of Fracture, 1–26. doi:10.1007/s10704-022-00685-5.

[34] 50-FMC Draft Recommendation. (1985). Determination of the fracture energy of mortar and concrete by means of three-point bend tests on notched beams. Materials and Structures, 18(4), 287–290. doi:10.1007/bf02472918.

[35] JCI-S-001e2003. (2003). Method of Test for Fracture Energy of Concrete by Use of Notched Beam. Japan Concrete Institute, Tokyo, Japan.

[36] Hanson, N. W., & Kurvits, O. A. (1965). Instrumentation for Structural Testing. Development Bulletin, 0144, 1-91.

[37] Bažant, Z. P., Yu, Q., & Zi, G. (2002). Choice of standard fracture test for concrete and its statistical evaluation. International Journal of Fracture, 118(4), 303–337. doi:10.1023/A:1023399125413.

[38] Bažant, Z. P., & Planas, J. (2019). Fracture and Size Effect in Concrete and Other Quasibrittle Materials. Routledge, New York, United States. doi:10.1201/9780203756799.

[39] Darwin, D., Barham, S., Kozul, R., & Luan, S., (2001). Fracture Energy of High-Strength Concrete. ACI Materials Journal, 98(5), 410-417.

[40] Rosselló, C., Elices, M., & Guinea, G. V. (2006). Fracture of model concrete: 2. Fracture energy and characteristic length. Cement and Concrete Research, 36(7), 1345–1353. doi:10.1016/j.cemconres.2005.04.016.

[41] IS456-2000 (2000) Indian Standard Plain and Reinforced Concrete Code of Practice. Bureau of Indian Standards, New Delhi, India.

[42] CEB-FIP Model Code. (2010). Final Draft. Federation Internationale Du Béton, Bulletins 65 & 66, Lausanne, Switzerland.

[43] ACI 318-19. (2022). Building Code Requirements for Structural Concrete and Commentary. American Concrete Institute (ACI), Michigan, United States.

[44] ACI 363R-92. (1997). State of the art report on high strength concrete. American Concrete Institute (ACI), Michigan, United States.

[45] Phillips, D. V., & Binsheng, Z. (1993). Direct tension tests on notched and un-notched plain concrete specimens. Magazine of Concrete Research, 45(162), 25–35. doi:10.1680/macr.1993.45.162.25.

[46] Hillerborg, A. R. N. E. (1983). Concrete fracture energy tests performed by 9 laboratories according to a draft RILEM recommendation. Report to RILEM TC50-FMC, Report TVBM-3015, Lund, Sweden.

[47] Hillerborg, A. (1985). Results of three comparative test series for determining the fracture energy GF of concrete. Materials and Structures, 18(5), 407–413. doi:10.1007/BF02472416.

[48] Comité Euro-International du Béton, (1990). CEB-FIP Model Code 1990. Thomas Telford, London, United Kingdom.

[49] Bažant, Z. P., Gettu, R., & Kazemi, M. T. (1991). Identification of nonlinear fracture properties from size effect tests and structural analysis based on geometry-dependent R-curves. International Journal of Rock Mechanics and Mining Sciences and, 28(1), 43–51. doi:10.1016/0148-9062(91)93232-U.

[50] Planas, J., Elices, M., & Guinea, G. V. (1992). Measurement of the fracture energy using three-point bend tests: Part 2-Influence of bulk energy dissipation. Materials and Structures, 25(5), 305–312. doi:10.1007/BF02472671.

[51] Strauss, A., Zimmermann, T., Lehký, D., Novák, D., & Keršner, Z. (2014). Stochastic fracture‐mechanical parameters for the performance‐based design of concrete structures. Structural Concrete, 15(3), 380-394. doi:10.1002/suco.201300077.

[52] Martin, J., Stanton, J., Mitra, N., & Lowes, L. N. (2007). Experimental testing to determine concrete fracture energy using simple laboratory test setup. ACI Materials Journal, 104(6), 575–584. doi:10.14359/18961.

[53] Khatieb, M. (2016). Experimental evaluation of concrete fracture energy and its dependency on relevant parameters. International Journal of Applied Engineering Research, 11(20), 10348–10352.

[54] Beygi, M. H. A., Kazemi, M. T., Nikbin, I. M., Vaseghi Amiri, J., Rabbanifar, S., & Rahmani, E. (2014). The influence of coarse aggregate size and volume on the fracture behavior and brittleness of self-compacting concrete. Cement and Concrete Research, 66, 75–90. doi:10.1016/j.cemconres.2014.06.008.

[55] Akram, A. (2021). The Overview of Fracture Mechanics Models for Concrete. Architecture, Civil Engineering, Environment, 14(1), 47–57. doi:10.21307/acee-2021-005.